Published in final edited form as:
Biochem J. ; 426(1): 31–41. doi:10.1042/BJ20091293.

Mitochondrial targeting of the electrophilic lipid 15-deoxy-Δ^{12,14}-Prostaglandin J_2 increases apoptotic efficacy via redox cell signaling mechanisms

Anne R. Diers[1,2], **Ashlee N. Higdon**[1,2], **Karina C. Ricart**[1,2], **Michelle S. Johnson**[1,2], **Anupam Agarwal**[1,3,4], **B. Kalyanaraman**[5], **Aimee Landar**[1,2], and **Victor M. Darley-Usmar**[1,2]

[1] Center for Free Radical Biology, University of Alabama at Birmingham, Birmingham, Alabama, USA 35294

[2] Department of Pathology, University of Alabama at Birmingham, Birmingham, Alabama, USA 35294

[3] Department of Medicine, University of Alabama at Birmingham, Birmingham, Alabama, USA 35294

[4] Nephrology Research and Training Center, University of Alabama at Birmingham, Birmingham, Alabama, USA 35294

[5] Department of Biophysics and Free Radical Research Center, Medical College of Wisconsin, Milwaukee, Wisconsin, USA 53226

SYNOPSIS

Prototypical electrophiles such as the lipid 15-deoxy-Δ^{12,14}-prostaglandin J_2 (15d-PGJ_2) are well recognized for their therapeutic potential. Electrophiles modify signaling proteins in both the cytosol and mitochondrion which results in diverse cellular responses including cytoprotective effects and, at high doses, cell death. These findings led us to the hypothesis that targeting electrophiles to specific compartments in the cell can be used to fine-tune their biological effects. To examine this, we synthesized a novel mitochondrially-targeted analog of 15d-PGJ_2 (mito-15d-PGJ_2) and tested its effects on redox cell signaling. Mito-15d-PGJ_2 caused profound defects in mitochondrial bioenergetics and mitochondrial membrane depolarization when compared to 15d-PGJ_2. We also found that mito-15d-PGJ_2 modified different members of the electrophile responsive proteome, was more potent at initiating intrinsic apoptotic cell death and was less effective than 15d-PGJ_2 at upregulating the expression of heme oxygenase-1 and glutathione. These data demonstrate the feasibility of modulating the biological effects of electrophiles by targeting the pharmacophore to mitochondria.

Keywords

15-deoxy-Δ^{12,14}-prostaglandin J_2; mitochondria; thiol; apoptosis; redox signaling

Corresponding author: Victor M. Darley-Usmar, Ph.D., Center for Free Radical Biology, Department of Pathology, University of Alabama at Birmingham, Biomedical Research Building II, 901 19th Street South, Birmingham, Alabama 35294, Tel: (205) 975-9686, Fax: (205) 934-7447, darley@uab.edu.

INTRODUCTION

Electrophilic compounds have attracted great interest as potential therapeutic agents in several fields including cancer, cardiovascular disease, and neurodegeneration [1–4]. Their primary mechanism of action occurs through their ability to covalently modify key proteins in redox cell signaling pathways [5–7]. Electrophiles can be derived from several sources including the diet, environment, or endogenously through enzymatic or non-specific lipid peroxidation processes [4,8]. Endogenously-generated electrophiles can be formed through enzymatic pathways, most notably cyclo-oxygenase. Arachidonic acid oxidation results in the formation of a family of lipid prostaglandins, some of which are electrophilic in nature [9,10]. These electrophilic cyclo-oxygenase metabolites have been shown to possess anti-cancer, anti-inflammatory, and cardioprotective properties [11–13].

Indeed, one of the best characterized electrophilic lipids generated from cyclo-oxygenase is 15-deoxy-$\Delta^{12,14}$-prostaglandin J_2 (15d-PGJ_2). It is particularly interesting because of its high degree of specificity for modification of protein cysteine residues (thiols) in signaling proteins [14]. For example, 15d-PGJ_2 has been shown to increase expression of phase II detoxification enzymes and cytoprotective intracellular antioxidants such as heme oxygenase-1 (HO-1) and the enzymes responsible for glutathione (GSH) synthesis [14–16]. Although, 15d-PGJ_2 is also known as a PPARγ agonist, the induction of HO-1 and GSH requires the presence of the electrophilic reactive center in the lipid and is not recapitulated by other non-reactive PPARγ agonist [15]. We have termed the highly selective family of proteins that form covalent adducts with electrophilic lipids the electrophile responsive proteome [17]. This is a discreet proteome since of the several hundred proteins in a cell which have potentially reactive thiols, approximately 10% form covalent protein adducts with 15d-PGJ_2.

In a therapeutic context, 15d-PGJ_2 has been proposed as both a potential anti-cancer and anti-inflammatory agent because of its ability to regulate redox-sensitive aspects of angiogenesis, growth arrest, expression of inflammatory cytokines and cell death in through the covalent modification of proteins [1,3]. For example, it has been shown to inhibit angiogenesis through the suppression of inflammatory enzymes and cytokines, and this occurs through the direct modification of key components of the nuclear factor kappa-light-chain-enhancer of activated B cells (NF-κ B) signaling pathway. Specifically, the potent anti-inflammatory effects of 15d-PGJ_2 are attributed to the covalent modification the p50 subunit of NF-κ B by 15d-PGJ_2 which results in the inhibition of its DNA binding activity [18]. Recently, it was found that 15d-PGJ_2 modifies two cysteine residues within the COOH-terminal zinc finger of ER-α, and this modification inhibits its DNA binding activity, decreases target gene expression, and inhibits proliferation [19]. The cell death effects of 15d-PGJ_2 which have been reported occur through a pleiotropic mechanism involving activation of PPARγ and through interactions with mitochondrial proteins which lead to the activation of apoptosis [12,20]. It is well recognized that these redox signaling pathways may be important therapeutic targets; however, the major limitation has been the inability to selectively target the specific redox signaling pathways which regulate the beneficial effects of electrophiles.

Evidence clearly supports the fact that protein targets of 15d-PGJ_2 in the electrophile responsive proteome are found in different compartments in the cell including the cytosol and mitochondria, and this is consistent with reports that 15d-PGJ_2 acts by pleiotropic mechanisms [18,21]. In work pioneered by Murphy et. al, a novel strategy for intracellular targeting of compounds to the mitochondrion has been developed. The conjugation of a delocalized, lipophilic cation to a compound of interest directs its accumulation within the mitochondrion and is sustained by the mitochondrial membrane potential [22,23]. This

strategy has been employed to direct therapeutic antioxidants to the mitochondrion [24–26]. Based on these previous studies suggesting that electrophilic modification of cytosolic targets are protective while modification of mitochondrial proteins may regulate apoptosis, we hypothesized that targeting an electrophile to the mitochondria would enhance the apoptotic effects of this compound while limiting the induction of intracellular antioxidants.

To test this hypothesis, we synthesized a novel mitochondrially-targeted analog of 15d-PGJ_2 (mito-15d-PGJ_2) and examined its effects on apoptotic cell death and induction of intracellular antioxidants. We found that mito-15d-PGJ_2 was more potent at initiating intrinsic apoptosis than 15d-PGJ_2. Additionally, mito-15d-PGJ_2 was less effective at upregulating Keap1-dependent antioxidant expression (HO-1 and GSH) and caused profound defects in mitochondrial bioenergetics and mitochondrial membrane depolarization when compared to 15d-PGJ_2. A mitochondrially-targeted analog of the non-electrophilic lipid prostaglandin E_2 (mito-PGE_2) and the targeting moiety methyltriphenylphosphonium (TPMP) did not recapitulate these effects. Taken together, these results demonstrate for the first time the feasibility of activating specific redox signaling pathways with an electrophile by selectively targeting specific compartments within the cell.

MATERIALS AND METHODS

Materials

All chemicals were of analytical grade and purchased from Sigma (St. Louis, MO) unless otherwise noted. 15d-PGJ_2 and prostaglandin E_2 were purchased from Cayman Chemical (Ann Arbor, MI). EZ-link 5-(biotinamido)pentylamine was purchased from Pierce (Rockford, IL) for the synthesis of biotinylated 15d-PGJ_2 (bt-15d-PGJ_2) as described previously [6]. Methyltriphenyl phosphonium bromide was used as a mitochondrial-targeting control. 2-amino-ethyl-triphenylphosphonium bromide was provided by Dr. B. Kalyanaraman.

Cell culture

MDA-MB231 human mammary adenocarcinoma cells were cultured in 10% fetal bovine serum (FBS) RPMI 1640 media (Cellgro). MCF10A immortalized human mammary epithelial cells were cultured in Mammary Epithelial Cell Growth Medium (MEGM) supplemented with MEGM SingleQuots (Lonza, Walkersville, MD). Murine embryonic fibroblasts (MEFs) derived from wild-type and Nrf2 $^{-\backslash -}$ mice as previously described [27] were cultured in 10% FBS DMEM media supplemented with 50 μM β-mercaptoethanol. All experiments using MDA-MB231 cells were performed in 0.5% FBS in RPMI 1640 media at ~50% confluence. Cells were cultured in 6-well cluster plates except for bioenergetic measurements in which case specialized Seahorse Bioscience culture plates (North Billerica, MA) were used. For lipid exposures in 6-well cluster plates, 1 mL media was used, and a 10 μM addition of lipid was then equivalent to ~160 pmols lipid/μg protein. For lipid exposures in Seahorse culture plates, 250 μL media was used, and a 10 μM addition of lipid was similar and approximately 125 pmols lipid/cell. Experiments utilizing MEFs and MCF10A cells were conducted at confluence in 0.5% FBS in DMEM or MEGM respectively with aforementioned supplementation.

Synthesis of mito-15d-PGJ_2 and mito-PGE_2

In order to target the lipids to the mitochondria, we utilized the lipophilic cation triphenylphosphonium (TPP+) [28]. The procedure is a modification of a previously reported method and is described in detail in the supplementary data section [6,29]. HPLC, UV-Visible spectral analysis, and mass spectrometric confirmation of synthesized lipids are

shown in Supplementary Figures 1–3. Structures for the parent compound and synthesized lipids are also shown in Figure 1.

Assessment of cell viability

After lipid exposure, aliquots of media from treatment wells were taken, and cells were harvested by scraping in PBS lysis buffer containing 0.1% Triton X-100. After centrifuging cell lysates to remove debris, lactate dehydrogenase (LDH) activity in supernatant and media aliquots was measured spectrophotometrically by monitoring the oxidation of NADH (0.3 mM) at 340 nm. Apoptosis and necrosis were measured after indicated treatment for 16 h by flow cytometric analysis using an Annexin V FITC Apoptosis Detection Kit (Calbiochem, San Diego, CA) using a BD LSR II flow cytometer. Briefly, gating parameters were set using propidium iodide (PI) only, Annexin V only, and no staining controls, and 10,000 events were collected for each experimental sample. Cells staining positive for both PI and Annexin V were considered late apoptotic. Cells staining positive for PI only or Annexin V only were scored as necrotic or early apoptotic respectively. Cells which stained negative for both PI and Annexin V were scored as viable cells.

Glutathione measurement

Total glutathione (glutathione + glutathione disulfide) was determined in cell lysates treated as indicated using the recycling assay described previously [30]. Briefly, after treatment, cells were lysed in 10 μM DTPA and 0.1% Triton X-100 in PBS, pH 7.4. Total glutathione in lysates was determined spectrophotometrically by monitoring the reduction of 5,5'-Dithio-bis(2-nitro-benzoic acid) at 412 nm. Values were normalized to protein content assayed by the Bradford method (Bio-Rad protein assay kit, Hercules, CA).

Western blot analysis

Cell lysate proteins were separated by 10% or 12.5% SDS-PAGE and transferred onto nitrocellulose membranes (Bio-Rad). Protein amounts were quantitated by the method of Bradford (Bio-Rad), and equivalent amounts of protein were loaded. Uniform protein loading was verified by Ponceau S staining of the membranes, which showed no significant differences in protein levels on the blots among samples. The membranes were blocked with 5% nonfat milk/TBS-T solution for 1 h at room temperature, and then incubated with primary antibody overnight at 4oC or for 3 h at room temperature. Antibody incubation conditions are as follows: anti-HO-1 (1:1000; Stressgen, Ann Arbor, MI), anti-caspase 9 (1:1000; Cell Signaling, Beverly, MA), anti-VDAC (1:3000; Mitosciences, Eugene, OR), anti-β-actin (1:1000; Cell Signaling) and anti-cytochrome *c* oxidase subunit I (1:1000; Mitosciences). After washing with TBS-T, membranes were incubated with a horseradish peroxidase (HRP)-conjugated secondary antibody (GE Healthcare, Piscataway, NJ). Membranes then were developed using SuperSignal West Dura chemiluminescence substrate (Pierce) and imaged using a CCD camera imaging system (AlphaInnotech, San Leandro, CA).

Measurement of mitochondrial function

To measure mitochondrial function in intact MDA-MB231 cells, a Seahorse Bioscience XF24 Extracellular Flux Analyzer was used [31]. The optimal seeding density of MDA-MB231 cells needed to obtain a measurable O_2 consumption and extracellular acidification rates (OCR and ECAR respectively) was established, and both ECAR and OCR show a proportional response with cell number (data not shown). For subsequent experiments a seeding density of 40,000 cells per well was selected to allow both potential increases and inhibition of OCR and ECAR to be assessed. We have noted that high levels of FCCP inhibit mitochondrial respiration presumably due to the loss of the ability to accumulate

respiratory substrates. Accordingly, oligomycin, FCCP, and antimycin A concentrations to elicit maximal effects were optimized in previous experiments (data not shown). The mitochondrial function assay employed in this study uses sequential injections of oligomycin, FCCP, and antimycin A to define a number of mitochondrial parameters such as basal OCR, ATP-linked OCR, proton leak, maximal respiratory capacity, reserve respiratory capacity, and non-mitochondrial oxygen consumption. It is important to note that in order to calculate these parameters, we have assumed that the oligomycin insensitive OCR is attributable to proton leak; however, oligomycin has been shown to hyperpolarize the mitochondrial membrane [32], and therefore, the resulting OCR is likely an upper estimate of the contribution from proton leak. The mitochondrial inner membrane electrochemical potential ($\Delta \psi$) was assessed using 5,5',6,6'-tetrachloro-1,1',3,3'-tetraethylbenzimidazolylcarbocyanine iodide (JC-1; Invitrogen, Carlsbad, CA). Briefly, cells grown in 12-well culture plates were treated as described in the figure legends, and JC-1 (7.4 μM) was added directly to MDA-MB231 cells in culture medium and incubated for 30 min. Next, cells were washed with PBS, and red/green fluorescence was measured using a fluorescence plate reader. Data are expressed as the ratio of red to green fluorescence.

Protein adduct detection and mitochondrial fractionation

Following experimental incubations, MDA-MB231 lysates were analyzed by two dimensional isoelectric focusing-SDS-PAGE. Total cell lysates (50 μg) were separated in the first dimension on a pH 3-10 gradient (IPG strips, Bio-Rad) followed by resolution on 12.5% SDS-polyacrylamide gels, and proteins were transferred to nitrocellulose membranes as described previously [15]. After blocking for 1 h, the membranes were probed using an anti-TPP+ antibody (1:10,000; received from Dr. Michael P. Murphy) with a HRP-conjugated secondary antibody and streptavidin conjugated to HRP (GE Healthcare) for detection of bt-15d-PGJ_2 and mito-15d-PGJ_2 adducts, respectively. Membranes were developed as described above, and total protein was detected using Deep Purple stain (GE Healthcare). Blots were analyzed using PDQuest software (Bio-Rad). For mitochondrial fractionation, after treatment, MDA-MB231 cells were harvested by scraping in ice-cold HMIM buffer (300 mM sucrose, 20 mM Tris-HCl, 2 mM EGTA, pH 7.35 at 4oC) containing protease inhibitors and PMSF (1 mM) as described in detail in the supplementary data. Protein adducts were detected using reagents described above. Membranes were developed using chemifluorescence detection and imaged using a Typhoon fluorescence detector (GE Healthcare,).

Statistical Analysis

Data reported are means ± s.e.m. for $n \geq 3$, as indicated in figure legends. Statistical significance was evaluated by one-way ANOVA among the groups using GraphPad Prism 4. The minimum level of significance was set at $p < 0.05$. Tukey's Multiple Comparisons test was used for post-hoc analysis of significance between groups.

RESULTS

Cytotoxicity of 15d-PGJ_2 and Mito-15d-PGJ_2

It is well established that lipid electrophiles at low concentrations induce phase II cytoprotective enzymes but at higher levels initiate cell death [16]. For example, the parent compound in these studies, 15d-PGJ_2, has been shown to induce apoptotic cell death in a number of cancer cell lines at doses ranging from 5–50 μM [33–35]. To assess cytotoxicity of mito-15d-PGJ_2 in human mammary cells, non-tumorigenic MCF10A mammary epithelial cells and MDA-MB231 mammary adenocarcinoma cells were exposed to mito-15d-PGJ_2 (3–30 μM, 16 h), and then cell death was assessed using LDH release as an indicator of late apoptotic or necrotic cell death. Treatment of both cell lines resulted in significant cell death

at concentrations at or above 10 μM (Fig. 2A). Additional examination of the cell death effects of mito-15d-PGJ_2 relative to 15d-PGJ_2 were conducted in MDA-MB231 cells. We next determined the relative cytotoxicity of mito-15d-PGJ_2 by treating MDA-MB231 cells with increasing concentrations (0.3–30μM) of either mito-15d-PGJ_2 or 15d-PGJ_2 for 16 h. Cytotoxicity was assessed using FACS analysis after staining with PI and Annexin V. Mito-15d-PGJ_2 treatment resulted in a greater decrease in viable cells (those that are not positive for either Annexin V or PI) at lower concentrations when compared to 15d-PGJ_2 (Fig. 2B). The percentage of early and late apoptotic cells were barely perceptible after exposure to 15d-PGJ_2 whereas this represented the majority of the populations with exposure to mito-15d-PGJ_2 (Fig. 2C,D). In contrast, 15d-PGJ_2 induced predominantly necrotic cell death at 30 μM whereas this represented only 3–10% of the cells treated with mito-15d-PGJ_2 across this dose range (Fig. 2E).

As a further confirmation that mito-15d-PGJ_2 causes apoptotic cell death, MDA-MB231 cells were treated with 10 μM 15d-PGJ_2 or mito-15d-PGJ_2 for 4 h, and then cell lysates were probed for procaspase 9, a protein which is cleaved upon the activation of the intrinsic (mitochondrial) apoptotic signaling. Treatment with 15d-PGJ_2 resulted in a partial loss, or activation, of procaspase 9 while mito-15d-PGJ_2 caused complete loss of this apoptotic mediator (Fig. 2F). Mito-PGE_2 and TPMP were used as controls for the effect of the triphenylphosphonium moiety and electrophilicity and had no effect on the levels of procaspase 9. Staurosporine (1 μM) was used as a positive control for caspase activation. Taken together these data show that mito-15d-PGJ_2 induces cell death primarily through apoptosis more robustly than 15d-PGJ_2 and is consistent with the hypothesis that mitochondrial-targeting then biases the mechanism of cell death towards apoptosis over necrosis.

Induction of the intracellular antioxidants HO-1 and GSH by 15d-PGJ_2 and mito-15d-PGJ_2

It has been shown that the modification of critical thiols in the cytosolic protein Keap1 by 15d-PGJ_2 results in translocation of the transcription factor nuclear factor erythroid 2-related factor 2 (Nrf2) to the nucleus and subsequent transcription of genes under the control of the Electrophile Response Element (EpRE) [15,36]. Such genes include HO-1 and subunits of the glutamyl cysteine ligase (GCL) which control the production of GSH [37]. Accordingly, we next investigated the effect of 15d-PGJ_2 and mito-15d-PGJ_2 on the induction of HO-1 and GSH. MDA-MB231 cells were treated with increasing concentrations (0.3–10 μM) of 15d-PGJ_2 or mito-15d-PGJ_2 for 4 h and cell lysates were analyzed for HO-1 protein levels. 15d-PGJ_2 caused a dose-dependent increase in HO-1 protein from 0.3-3 μM then a slight decrease at higher concentrations (Fig. 3A) similar to the biphasic dose response we have previously described [16]. However, mito-15d-PGJ_2 induced HO-1 to a much lesser extent. TPMP (10 μM) was used as a control for the effect of the triphenylphosphonium moiety and had no effect on HO-1 levels.

As an additional readout of the effect of the electrophiles on the Keap1/Nrf2 system, GSH was also assessed by treating MDA-MB231 cells (4 h) with increasing concentrations (0.3–10 μM) of 15d-PGJ_2 or mito-15d-PGJ_2. Compound containing media was then removed to attenuate cytotoxicity, and the cells incubated for a further 16 h to allow time for the *de novo* synthesis of GSH. Similar to the result with HO-1, 15d-PGJ_2 treatment resulted in a significant increase in total GSH levels; however, mito-15d-PGJ_2 was unable to induce GSH (Fig. 3B).

Nrf2 dependence of the regulation of antioxidant expression and cell death by 15d-PGJ_2

We have previously reported that the induction of HO-1 by 15d-PGJ_2 can be inhibited by modification of mitochondrial protein thiols [16]. To test the possibility that mito-15d-PGJ_2

is functioning through a similar mechanism, cells were pretreated with mito-15d-PGJ_2 for 4 h then 15d-PGJ_2 was added to stimulate HO-1 and GSH levels. Mito-15d-PGJ_2 does not impair 15d-PGJ_2 induction of HO-1 indicating that is not inhibiting the mitochondrial component required for HO-1 synthesis (Fig. 4A). Interestingly, in the combined treatment group, mito-15d-PGJ_2 pretreatment enhances HO-1 induction by 15d-PGJ_2. These data are consistent with the known ability of HO-1 to be induced by a number of mechanisms some of which appear to be independent of Keap1/Nrf2 [38]. In contrast, the induction of GSH appears to require Nrf2 and consistent with this finding, pretreatment with mito-15d-PGJ_2 does not impair 15d-PGJ_2-dependent induction of GSH (Fig. 4B).

It has been established that activation of the Keap1/Nrf2 system by low levels of electrophilic stress results increased resistance to cytotoxic levels of reactive oxygen and nitrogen species. It is then possible that the failure of mito-15d-PGJ_2 to activate the EpRE may contribute to its cytotoxicity. To test this, two different experimental strategies were employed. First, MDA-MB231 cells were co-incubated with a cell death-inducing concentration of mito-15d-PGJ_2 (10 μM) and a concentration of 15d-PGJ_2 which increases antioxidant expression (3 μM). After 16 h treatment, cell death was assessed by LDH release and was unchanged by co-treatment with 15d-PGJ_2 (Fig. 4C). This is consistent with the early induction of the apoptotic process before significant induction of phase II cytoprotective enzymes can occur. Secondly, wild-type and Nrf2 $^{-/-}$ murine embryonic fibroblasts were treated with 10 μM 15d-PGJ_2 or mito-15d-PGJ_2 and cell death was assessed. If the cytotoxicity is attenuated by activation of the Keap1/Nrf2 system, we would expect Nrf2 null cells to be sensitized to the electrophiles; however, we found that cytotoxicity of 15d-PGJ_2 and mito-15d-PGJ_2 is independent of Nrf2 levels in the cell (Fig. 4D).

Protein modification by bt-15d-PGJ_2 and mito-15d-PGJ_2 differ

The data thus far demonstrating the different biological properties of 15d-PGJ_2 and mito-15d-PGJ_2 suggest that the proteins modified by the electrophilic lipids will also differ. To test this, MDA-MB231 cells were incubated with bt-15d-PGJ_2 or mito-15d-PGJ_2 (10 μM) for 1 h, and the protein lysates separated by 2D-IEF-SDS-PAGE followed by western blotting and detection for protein-lipid adducts using the TPP+ antibody or streptavidin conjugated to HRP. The patterns of protein stains for all treatments showed no significant differences (result not shown). Control cells not treated with electrophilic lipid showed no major positive reactions with the exception of one spot on the biotin blot (Fig. 5A,B) which we ascribe to an endogenous biotin containing carboxylase [6]. Figure 5 shows detection of approximately 63 proteins positive for biotin (panel C) and approximately 32 proteins positive for TPP (Panel D). The images were selected to minimize differences in potential sensitivity between the two detection techniques by selecting images with the same intensity for a common spot (indicated by an arrow on Fig. 5C) The overlay of these two images was achieved using the PDQuest proteomics software (Fig. 5E) and shows red spots that are predominantly reactive with bt-15d-PGJ_2 and green spots with mito-15d-PGJ_2, and the proteins that react with both lipids are yellow. In Figure 5F, these data are summarized and indicate that 10 proteins are common targets of both electrophilic lipids, with 22 unique to mito-15d-PGJ_2 and 53 unique to 15d-PGJ_2. It was not possible to unequivocally overlay the protein adduct maps with the protein stain to identify these targets since many of these proteins are present in the cell at low abundance [6].

15d-PGJ_2 and mito-15d-PGJ_2 localize to mitochondria and affect mitochondrial membrane potential

To assess the relative localization and formation of protein adducts by the lipid electrophiles, mitochondrial fractions were isolated from cells treated with bt-15d-PGJ_2 or

mito-15d-PGJ_2. Validation of the fractionation protocol used demonstrates substantial enrichment of the mitochondrial proteins in the mitochondrial fraction compared to the cytosolic fraction (Supplementary Fig. 4).

Protein adduct formation was assessed in fractionated samples from bt-15d-PGJ_2 and mito-15d-PGJ_2 treated cells using 1D-SDS-PAGE. Consistent with our previous results, bt-15d-PGJ_2 localizes to the mitochondria and forms stable protein adducts [21]. Mito- 15d-PGJ_2 protein adducts are also enriched in the mitochondrial fraction (Fig. 6A). Mitochondrial purity was also confirmed by VDAC enrichment in the mitochondrial fraction. Protein adducts in each fraction were quantified and expressed as fold increase in protein adducts in the mitochondrial fraction compared with the homogenate (Fig. 6B). These data demonstrate that there is a significant increase in mito-15d-PGJ_2 protein adducts in the mitochondria compared to the homogenate. There was also a trend towards an increase in mitochondrial protein adducts with bt-15d-PGJ_2 treatment, however, this result was not significant.

We next investigated whether the modification of mitochondrial proteins by lipid electrophiles altered mitochondrial function by determining the effect of 15d-PGJ_2 and mito-15d-PGJ_2 on mitochondrial membrane potential ($\Delta\psi$). MDA-MB231 cells were treated for 4 h with increasing concentrations (1–10 μM) of 15d-PGJ_2 or mito-15d-PGJ_2 then JC-1 fluorescence was assessed. Treatment with 15d-PGJ_2 resulted in a dose-dependent decrease in the mitochondrial membrane potential. However, mito-15d-PGJ_2 caused a more significant depolarization of the mitochondrial membrane (Fig. 6C). TPMP was used as a control for the effect of the triphenylphosphonium moiety and did not cause mitochondrial membrane depolarization.

Measurement of mitochondrial function after exposure to 15d-PGJ_2 and mito-15d-PGJ_2

To assess cellular bioenergetics in intact MDA-MB231 cells, the Seahorse Bioscience XF24 extracellular flux analyzer was used to determine the rates of change in both pH and oxygen in the media surrounding the cells [31,39]. We have utilized a mitochondrial function protocol which is schematically represented in Fig. 7A. This protocol is a modification of one described previously [40]. Initially, basal oxygen consumption rate (OCR) is measured, and after 20 min, the inhibitor of the mitochondrial ATP synthase, oligomycin (0.3 μg/mL) is added. This results in a decrease in OCR which we ascribe to the mitochondrial activity utilized for ATP synthesis. The remaining OCR can be ascribed to all processes which allow ion movement across the mitochondrial inner membrane, and we collectively term this proton leak. Next, the maximal mitochondrial function that can be sustained in the cells with endogenous substrates is assessed by the addition of the proton ionophore, FCCP (1 μM). As expected, this stimulates oxygen consumption, as it is no longer constrained by the proton gradient in the mitochondria. The difference between the basal OCR and this maximal rate is then termed the reserve capacity of the mitochondrial function in the cells under these conditions. Finally, the complex III inhibitor antimycin A is added to assess the oxygen consumption at cytochrome *c* oxidase, the terminal member of the electron transport chain. The low level of remaining OCR can be ascribed to partial reduction of oxygen and is therefore ascribed to reactive oxygen species (ROS) formation.

Using this protocol, mitochondrial function was measured in confluent MDA-MB231 cells which were first exposed to 15d-PGJ_2, mito-15d-PGJ_2 or mito-PGE_2 (10 μM, 30 min). The lipids were then removed and the mitochondrial parameters measured. There was no significant effect of 15d-PGJ_2 or mito-PGE_2 on basal or maximal respiration; however, profound decreases in basal and maximal OCR were seen with mito-15d-PGJ_2 treatment (Fig. 7B,C). The analysis of the different components of OCR as described above were also calculated and shown (Fig. 7D). It is clear that 15d-PGJ_2 has little effect on mitochondrial

function whereas mito-15d-PGJ_2 suppresses all bioenergetic parameters. In addition to the measurement of OCR, the extracellular acidification rate (ECAR), a surrogate marker of glycolysis, was also determined (Fig. 7E). Under unstimulated conditions, ECAR represents predominantly lactate production from glycolysis. Treatment with either 15d-PGJ_2 or mito-PGE_2 resulted in no change in ECAR; however, after a 30 min exposure to mito-15d-PGJ_2, ECAR is significantly increased. It is important to note that at this time point apoptosis has not yet been activated (Fig. 7F); thus, these mitochondrial bioenergetic defects precede apoptosis. Taken together these data show that mito-15d-PGJ_2 modifies mitochondrial function whereas 15d-PGJ_2 has a minimal effect on any of the bioenergetic parameters assessed. Moreover, glycolytic flux as indicated by elevated ECAR is increased with mito-15d- PGJ_2 which may represent a compensatory mechanism to overcome lost mitochondrial function.

DISCUSSION

The control of redox signaling in cells is now emerging as a key area for our understanding of both the etiology of disease and the development of novel therapeutics. It is well recognized that redox signaling offers potential therapeutic targets; however, the major limitation has been the inability to selectively activate or inhibit a specific pathway [41]. To our knowledge, this is the first demonstration of selective targeting of a redox signaling pathway by modifying an electrophilic lipid to target the mitochondrion. We selected the compound 15d-PGJ_2 for these studies because of its recognized potential as a therapeutic agent and its well established ability to modify proteins and activate cell signaling in both the cytosol and mitochondrion. We have demonstrated that by conjugating the delocalized cation TPP+ to 15d-PGJ_2 we are able to enhance its cytotoxicity by promoting apoptosis over necrosis when compared to the parent compound (Fig. 2). It is likely that the mechanism through which this occurs is the covalent modification of proteins since the non-electrophilic lipid analog to mito-15d-PGJ_2, mito-PGE_2, has no effect on cell death or caspase 9 activation. There are multiple potential mechanisms by which mito-15d-PGJ_2 could enhance apoptosis in cells. It is unlikely that mito-15d-PGJ_2 activates PPARγ-dependent cell death since PPARγ is localized primarily in the cytosol and blocking the COOH functional group on the lipid leads to loss of its PPARγ-dependent properties [42,43].

Since mito-15d-PGJ_2 is added to the outside to the cell it will accumulate first in the cytosol based upon the membrane potential across the plasma membrane and only then will cross the inner mitochondrial membrane and accumulate in the mitochondrion [22,44]. Consistent with this model, we found that the protein adducts presented a distinct pattern when separated by 2D-IEF-SDS-PAGE. As expected, the proteome for the mito-15d-PGJ_2 shares some common targets with 15d-PGJ_2, but a far greater number of proteins (53 for bt-15d-PGJ_2 and 22 for mito-15d-PGJ_2) are distinct (Fig. 5). The fact that mito-15d-PGJ_2 has substantially fewer protein targets is consistent with our hypothesis that the sub-proteomes modified by reactive electrophiles are cell domain specific. There are, however, some limitations to this analysis of the electrophilic proteome. For example, not all the proteins which are modified are capable of entering the second dimension of the 2D-IEF-SDS-PAGE due to precipitation in the isoelectric strip (result not shown). Nevertheless, it is clear from those proteins that are represented that the patterns are distinct. Moreover, as expected, modified proteins were present in both the cytosolic and mitochondrial fractions of cells exposed to both mito-15d-PGJ_2 and the untargeted analog (Fig. 6). Fractionation of the cells after exposure to the electrophiles resulted in a greater enrichment of adducted proteins relative to the unfractionated sample for mito-15d-PGJ_2 compared to 15d-PGJ_2. In further support of a selective impact on mitochondrial function by the addition of the TPP+ group to 15d-PGJ_2, we found that mito-15d-PGJ_2 caused a profound mitochondrial defect in

oxidative phosphorylation at concentrations where 15d-PGJ_2 had no discernable effect (Fig. 7).

There are several potential mechanisms for the increased toxicity of mito-15d-PGJ_2. Firstly, mito-15d-PGJ_2 may more extensively modify mitochondrial targets of the parental compound, 15d-PGJ_2. We have previously reported that 15d-PGJ_2 modifies components of the mitochondrial permeability transition pore including the adenine nucleotide translocator (ANT) and promotes permeability transition in endothelial cells [20]. There is also the potential that mito-15d-PGJ_2 enhances cell death by limiting the cytoprotective response of cells to the electrophilic stress they experience. Nrf2-dependent gene transcription results in an increase in the overall antioxidant capacity of cells and has recently been demonstrated to also initiate anti-apoptotic responses [45]. A last potential mechanism for increased cytotoxicity of mito-15d-PGJ_2 maybe through the modification of new mitochondrial protein targets as a result of targeting 15d-PGJ_2. Our data suggest that the loss of Nrf2-dependant gene transcription does not explain the enhanced cytotoxicity of mito-15d-PGJ_2 (Fig. 4). Co-incubation of an Nrf2-activating concentration of 15d-PGJ_2 does not protect against mito-15d-PGJ_2 induced cell death. Moreover, wild-type and $Nrf^{-/-}$ murine embryonic fibroblasts have similar cytotoxicity profiles pointing to the fact that Nrf2 is not a key mediator of the cell death phenotype on acute exposure to an electrophile. However, it is important to note that induction of antioxidant defenses with low non-toxic concentrations of electrophiles has been shown to be essential for the protection against a subsequent oxidative stress [46].

The fact that the loss of Nrf2 signaling does not appear to be a mediator of the enhanced cell death effects of mito-15d-PGJ_2, does not preclude the role of mitochondrial thiol modification as a mechanism. We have demonstrated that both mito-15d-PGJ_2 and 15d-PGJ_2 localize to the mitochondrion and in 2D protein adduct formation analysis, we have identified a number of common protein targets of the two compounds, likely the cell death targets (Fig. 5,6). Interestingly, we also show that mito-15d-PGJ_2 has profound effects on mitochondrial bioenergetics that are not observed with untargeted 15d-PGJ_2 (Fig. 7). These data suggest a potential role for both the extent of modification of common targets and a gain-of-function activity of mito-15d-PGJ_2 through the modification of unique mitochondrial protein targets that results in impaired mitochondrial respiration and may contribute to cell death. Consistent with this idea, our data also demonstrate that concentrations at which mitochondrial function is impaired are also those which are required to initiate apoptosis.

We reasoned that if mito-15d-PGJ_2 was accumulated in the mitochondrion it would be less effective at activating cytosolic signaling pathways. To test this we chose to measure the initiation of EpRE-dependant genes such as HO-1 or the proteins controlling GSH synthesis by the electrophilic lipids [37]. We found that the ability of mito-15d-PGJ_2 to upregulate HO-1 is greatly attenuated and for GSH is essentially abolished when compared to 15d-PGJ_2 (Fig. 3).

Here, we have demonstrated the feasibility of targeting specific cell responses by targeting a subcellular proteome (the mitochondrion). We successfully targeted the cellular response of cell death and selected against another (antioxidant upregulation). It is important to note that the addition of the TPP+ moiety to 15d-PGJ_2 may impact on the electrophilic responsive proteome through mechanisms distinct from mitochondrial targeting. For example, it likely changes the lipophilicity of the parent electrophile and may also provide additional steric factors which change the reactivity to target proteins. Taken together these data indicate that both the reactivity of the thiol proteome and the physical-chemical properties of the electrophile will determine the specific electrophile responsive sub-proteomes which are

modified and thus the biological responses. This has important implications for both the understanding of the basic mechanisms through which electrophiles mediate redox cell signaling and the potential to refine the protein targets of electrophiles through intracellular targeting strategies.

Supplementary Material

Refer to Web version on PubMed Central for supplementary material.

Acknowledgments

This research was supported by NIH grants ES10167, DK 75865, (VDU), DK 079337 (AA), T32 HL007918 (ARD), and American Heart Association funding through the Scientist Development Grant 0635361N (AL), and Predoctoral Fellowship 0815177E (ANH). We are grateful to Jeffrey Chan for the Nrf2 wild type and knockout mouse embryonic fibroblasts and to Michael Murphy for the TPP+ antibody.

The abbreviations used are

15d-PGJ$_2$	15-deoxy-$\Delta^{12,14}$-prostaglandin J$_2$
Δ ψ	mitochondrial membrane potential
ANT	adenine nucleotide translocator
bt-15d-PGJ$_2$	biotinylated 15d-PGJ$_2$
COX	cytochrome *c* oxidase
ECAR	extracellular acidification rate
EpRE	Electrophile Response Element
ER-α	estrogen receptor alpha
FBS	fetal bovine serum
FCCP	carbonyl cyanide 4-(trifluoromethoxy)phenylhydrazone
GCL	glutamyl cysteine ligase
GSH	glutathione
HO-1	heme oxygenase-1
HSP70	heat shock protein 70
IEF	isoelectric focusing
JC-1	5,5',6,6'-tetrachloro-1,1',3,3'-tetraethylbenzimidazolylcarbocyanine iodide
Keap1	Kelch-like ECH-associated protein 1
LDH	lactate dehydrogenase
MEFs	murine embryonic fibroblasts
mito-15d-PGJ$_2$	mito-15-deoxy-$\Delta^{12,14}$-prostaglandin J$_2$
mito-PGE$_2$	mito-prostaglandin E$_2$
NF-κ B	nuclear factor kappa-light-chain-enhancer of activated B cells
Nrf2	factor nuclear factor erythroid 2-related factor 2
OCR	oxygen consumption rate

PI	propidium iodide
PPARγ	peroxisome proliferator-activated receptor gamma
TBS-T	Tris buffered saline with Tween
TPMP	methyltriphenylphosphonium
TPP+	triphenylphosphonium
VDAC	voltage dependent anion channel

References

1. Conti M. Cyclopentenone: a special moiety for anticancer drug design. Anticancer Drug. 2006; 17:1017–1022.
2. Na HK, Surh YJ. Peroxisome proliferator-activated receptor gamma (PPARgamma) ligands as bifunctional regulators of cell proliferation. Biochem Pharmacol. 2003; 66:1381–1391. [PubMed: 14555212]
3. Straus DS, Glass CK. Cyclopentenone prostaglandins: New insights on biological activities and cellular targets. Med Res Rev. 2001; 21:185–210. [PubMed: 11301410]
4. Satoh T, Lipton SA. Redox regulation of neuronal survival mediated by electrophilic compounds. Trends Neurosci. 2007; 30:37–45. [PubMed: 17137643]
5. Stamatakis K, Perez-Sala D. Prostanoids with Cyclopentenone Structure as Tools for the Characterization of Electrophilic Lipid-Protein Interactomes. Ann NY Acad Sci. 2006; 1091:548–570. [PubMed: 17341644]
6. Landar A, Oh JY, Giles NM, Isom A, Kirk M, Barnes S, Darley-Usmar VM. A sensitive method for the quantitative measurement of protein thiol modification in response to oxidative stress. Free Radic Biol Med. 2006; 40:459–468. [PubMed: 16443161]
7. Perez-Sala D, Cernuda-Morollon E, Canada FJ. Molecular basis for the direct inhibition of AP-1 DNA binding by 15-deoxy-Delta 12,14-prostaglandin J2. J Biol Chem. 2003; 278:51251–51260. [PubMed: 14532268]
8. Liebler DC. Protein damage by reactive electrophiles: targets and consequences. Chem Res Toxicol. 2008; 21:117–128. [PubMed: 18052106]
9. Lands WE. The biosynthesis and metabolism of prostaglandins. Annu Rev Physiol. 1979; 41:633–652. [PubMed: 219768]
10. Shibata T, Kondo M, Osawa T, Shibata N, Kobayashi M, Uchida K. 15-deoxy-delta 12,14-prostaglandin J2. A prostaglandin D2 metabolite generated during inflammatory processes. J Biol Chem. 2002; 277:10459–10466. [PubMed: 11786541]
11. Gilroy DW, Colville-Nash PR, Willis D, Chivers J, Paul-Clark MJ, Willoughby DA. Inducible cyclooxygenase may have anti-inflammatory properties. Nat Med. 1999; 5:698–701. [PubMed: 10371510]
12. Pignatelli M, Sanchez-Rodriguez J, Santos A, Perez-Castillo A. 15-deoxy-Delta-12,14-prostaglandin J2 induces programmed cell death of breast cancer cells by a pleiotropic mechanism. Carcinogenesis. 2005; 26:81–92. [PubMed: 15485993]
13. Blanco M, Moro MA, Davalos A, Leira R, Castellanos M, Serena J, Vivancos J, Rodriguez-Yanez M, Lizasoain I, Castillo J. Increased plasma levels of 15-deoxyDelta prostaglandin J2 are associated with good outcome in acute atherothrombotic ischemic stroke. Stroke; a journal of cerebral circulation. 2005; 36:1189–1194.
14. Oh JY, Giles N, Landar A, Darley-Usmar V. Accumulation of 15-deoxy-delta(12,14)-prostaglandin J2 adduct formation with Keap1 over time: effects on potency for intracellular antioxidant defence induction. Biochem J. 2008; 411:297–306. [PubMed: 18237271]
15. Levonen AL, Landar A, Ramachandran A, Ceaser EK, Dickinson DA, Zanoni G, Morrow JD, Darley-Usmar VM. Cellular mechanisms of redox cell signalling: role of cysteine modification in

controlling antioxidant defences in response to electrophilic lipid oxidation products. Biochem J. 2004; 378:373–382. [PubMed: 14616092]

16. Ricart KC, Bolisetty S, Johnson MS, Perez J, Agarwal A, Murphy MP, Landar A. The permissive role of mitochondria in the induction of haem oxygenase-1 in endothelial cells. Biochem J. 2009; 419:427–436. [PubMed: 19161347]
17. Ceaser EK, Moellering DR, Shiva S, Ramachandran A, Landar A, Venkartraman A, Crawford J, Patel R, Dickinson DA, Ulasova E, Ji S, Darley-Usmar VM. Mechanisms of signal transduction mediated by oxidized lipids: the role of the electrophile-responsive proteome. Biochem Soc Trans. 2004; 32:151–155. [PubMed: 14748737]
18. Cernuda-Morollon E, Pineda-Molina E, Canada FJ, Perez-Sala D. 15-Deoxy-Delta 12,14-prostaglandin J2 Inhibition of NF-kappa B-DNA Binding through Covalent Modification of the p50 Subunit. J Biol Chem. 2001; 276:35530–35536. [PubMed: 11466314]
19. Kim HJ, Kim JY, Meng Z, Wang LH, Liu F, Conrads TP, Burke TR, Veenstra TD, Farrar WL. 15-Deoxy-{Delta}12,14-Prostaglandin J2 Inhibits Transcriptional Activity of Estrogen Receptor-{alpha} via Covalent Modification of DNA-Binding Domain. Cancer Res. 2007; 67:2595–2602. [PubMed: 17363578]
20. Landar A, Shiva S, Levonen AL, Oh JY, Zaragoza C, Johnson MS, Darley-usmar VM. Induction of the permeability transition and cytochrome c release by 15-deoxy-Delta12,14-prostaglandin J2 in mitochondria. Biochem J. 2006; 394:185–195. [PubMed: 16268779]
21. Landar A, Zmijewski JW, Dickinson DA, Le Goffe C, Johnson MS, Milne GL, Zanoni G, Vidari G, Morrow JD, Darley-Usmar VM. Interaction of electrophilic lipid oxidation products with mitochondria in endothelial cells and formation of reactive oxygen species. Am J Physiol Heart Circ Physiol. 2006; 290:H1777–1787. [PubMed: 16387790]
22. Smith RAJ, Porteous CM, Gane AM, Murphy MP. Delivery of bioactive molecules to mitochondria invivo. Proc Natl Acad Sci. 2003; 100:5407–5412. [PubMed: 12697897]
23. Ross MF, Da Ros T, Blaikie FH, Prime TA, Porteous CM, Severina II, Skulachev VP, Kjaergaard HG, Smith RA, Murphy MP. Accumulation of lipophilic dications by mitochondria and cells. Biochem J. 2006; 400:199–208. [PubMed: 16948637]
24. Smith RAJ, Porteous CM, Coulter CV, Murphy MP. Selective targeting of an antioxidant to mitochondria. Euro J Biochem. 1999; 263:709–716.
25. Jauslin ML, Meier T, Smith RA, Murphy MP. Mitochondria-targeted antioxidants protect Friedreich Ataxia fibroblasts from endogenous oxidative stress more effectively than untargeted antioxidants. Faseb J. 2003; 17:1972–1974. [PubMed: 12923074]
26. Lowes DA, Thottakam BMV, Webster NR, Murphy MP, Galley HF. The mitochondria-targeted antioxidant MitoQ protects against organ damage in a lipopolysaccharide-peptidoglycan model of sepsis. Free Radic Biol Med. 2008; 45:1559–1565. [PubMed: 18845241]
27. Leung L, Kwong M, Hou S, Lee C, Chan JY. Deficiency of the Nrf1 and Nrf2 transcription factors results in early embryonic lethality and severe oxidative stress. J Biol Chem. 2003; 278:48021–48029. [PubMed: 12968018]
28. Murphy MP, Smith RAJ. Targeting Antioxidants to Mitochondria by Conjugation to Lipophilic Cations. Annu Rev Pharmacol Toxicol. 2007; 47:629–656. [PubMed: 17014364]
29. Higdon AN, Dranka BP, Hill BG, Oh JY, Johnson MS, Landar A, Darley-Usmar VM. Methods for imaging and detecting modification of proteins by reactive lipid species. Free Radic Biol Med. 2009; 47:201–212. [PubMed: 19446632]
30. Tietze F. Enzymatic Method for Quantitative Determination of Nanogram Amounts of Total and Oxidized Glutathione: Applications to Mammalian Blood and Other Tissues. Anal Biochem. 1969; 27:502–522. [PubMed: 4388022]
31. Ferrick DA, Neilson A, Beeson C. Advances in measuring cellular bioenergetics using extracellular flux. Drug Discov Today. 2008; 13:268–274. [PubMed: 18342804]
32. Nicholls DG, Ward MW. Mitochondrial membrane potential and neuronal glutamate excitotoxicity: mortality and millivolts. Trends Neurosci. 2000; 23:166–174. [PubMed: 10717676]
33. Moriai M, Tsuji N, Kobayashi D, Kuribayashi K, Watanabe N. Down-regulation of hTERT expression plays an important role in 15-deoxy-Delta12,14-prostaglandin J2-induced apoptosis in cancer cells. Int J Oncol. 2009; 34:1363–1372. [PubMed: 19360348]

34. Qiao L, Dai Y, Gu Q, Chan KW, Zou B, Ma J, Wang J, Lan HY, Wong BC. Down-regulation of X-linked inhibitor of apoptosis synergistically enhanced peroxisome proliferator-activated receptor gamma ligand-induced growth inhibition in colon cancer. Mol Cancer Ther. 2008; 7:2203–2211. [PubMed: 18645029]
35. Han H, Shin SW, Seo CY, Kwon HC, Han JY, Kim IH, Kwak JY, Park JI. 15-Deoxy-Δ12,14-prostaglandin J2 (15d-PGJ2) sensitizes human leukemic HL-60 cells to tumor necrosis factor-related apoptosis-inducing ligand (TRAIL)-induced apoptosis through Akt downregulation. Apoptosis. 2007; 12:2101–2114. [PubMed: 17786557]
36. Tong KI, Kobayashi A, Katsuoka F, Yamamoto M. Two-site substrate recognition model for the Keap1-Nrf2 system: a hinge and latch mechanism. Biol Chem. 2006; 387:1311–1320. [PubMed: 17081101]
37. Kobayashi M, Yamamoto M. Molecular mechanisms activating the Nrf2-Keap1 pathway of antioxidant gene regulation. Antioxid Redox Signal. 2005; 7:385–394. [PubMed: 15706085]
38. Hock TD, Liby K, Wright MM, McConnell S, Schorpp-Kistner M, Ryan TM, Agarwal A. JunB and JunD regulate human heme oxygenase-1 gene expression in renal epithelial cells. J Biol Chem. 2007; 282:6875–6886. [PubMed: 17204476]
39. Wu M, Neilson A, Swift AL, Moran R, Tamagnine J, Parslow D, Armistead S, Lemire K, Orrell J, Teich J, Chomicz S, Ferrick DA. Multiparameter metabolic analysis reveals a close link between attenuated mitochondrial bioenergetic function and enhanced glycolysis dependency in human tumor cells. Am J Physiol Cell Physiol. 2007; 292:C125–136. [PubMed: 16971499]
40. Jekabsons MB, Nicholls DG. In situ respiration and bioenergetic status of mitochondria in primary cerebellar granule neuronal cultures exposed continuously to glutamate. J Biol Chem. 2004; 279:32989–33000. [PubMed: 15166243]
41. Trachootham D, Lu W, Ogasawara MA, Nilsa RD, Huang P. Redox regulation of cell survival. Antioxid Redox Signal. 2008; 10:1343–1374. [PubMed: 18522489]
42. Sanchez-Gomez FJ, Cernuda-Morollon E, Stamatakis K, Perez-Sala D. Protein thiol modification by 15-deoxy-Delta12,14-prostaglandin J2 addition in mesangial cells: role in the inhibition of pro-inflammatory genes. Mol Pharmacol. 2004; 66:1349–1358. [PubMed: 15317873]
43. Shiraki T, Kamiya N, Shiki S, Kodama TS, Kakizuka A, Jingami H. Alpha,beta-unsaturated ketone is a core moiety of natural ligands for covalent binding to peroxisome proliferator-activated receptor gamma. J Biol Chem. 2005; 280:14145–14153. [PubMed: 15695504]
44. Burns RJ, Smith RAJ, Murphy MP. Synthesis and Characterization of Thiobutyltriphenylphosphonium Bromide, a Novel Thiol Reagent Targeted to the Mitochondrial Matrix. Arch Biochem Biophys. 1995; 322:60–68. [PubMed: 7574695]
45. Lau A, Villeneuve NF, Sun Z, Wong PK, Zhang DD. Dual roles of Nrf2 in cancer. Pharmacol Res. 2008; 58:262–270. [PubMed: 18838122]
46. Moellering DR, Levonen AL, Go YM, Patel RP, Dickinson DA, Forman HJ, Darley-Usmar VM. Induction of glutathione synthesis by oxidized low-density lipoprotein and 1-palmitoyl-2-arachidonyl phosphatidylcholine: protection against quinone-mediated oxidative stress. Biochem J. 2002; 362:51–59. [PubMed: 11829739]

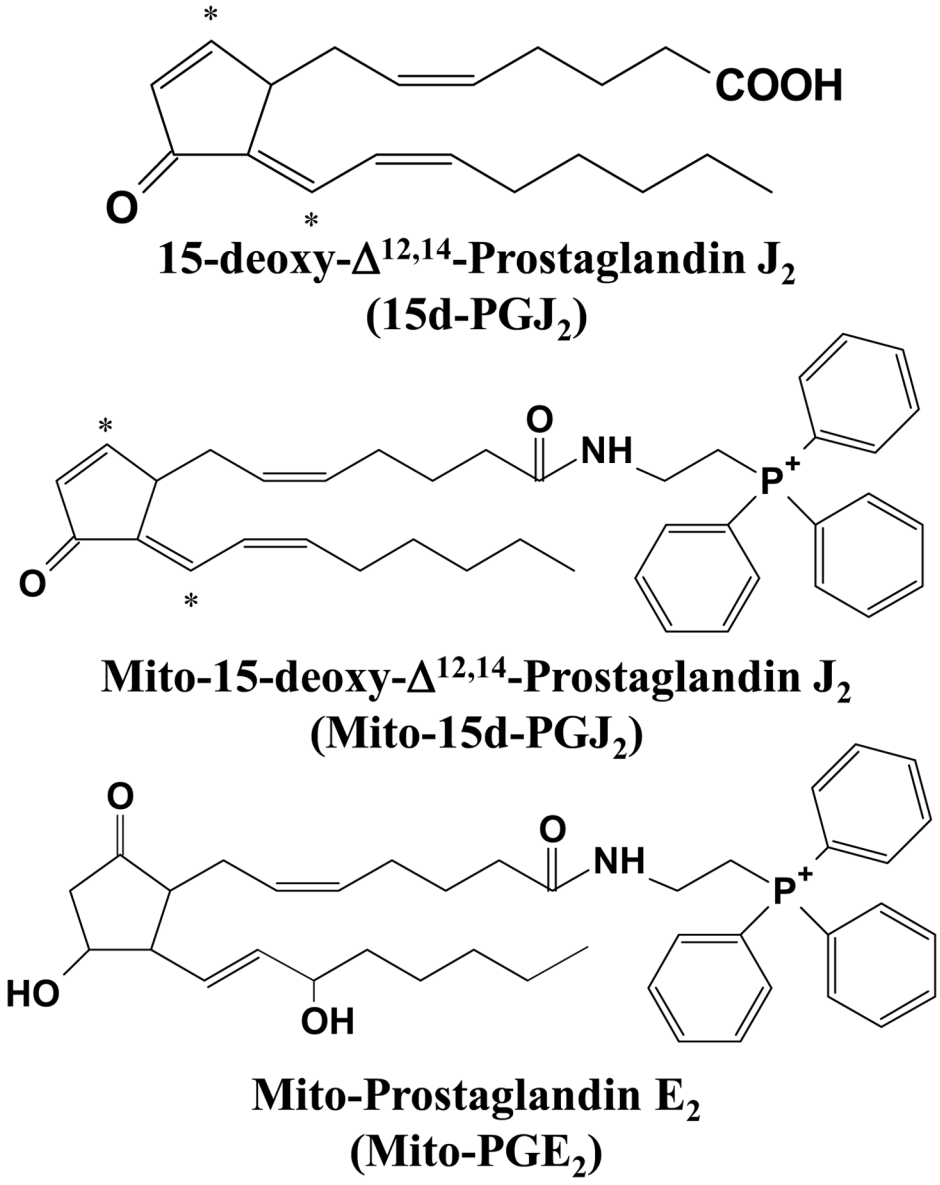

Figure 1. Structures of lipids

Structures of 15d-PGJ_2 and the mitochondrially targeted lipids derivatives mito-15d-PGJ_2 and mito-PGE_2 are shown. Electrophilic carbon centers are denoted with asterisks.

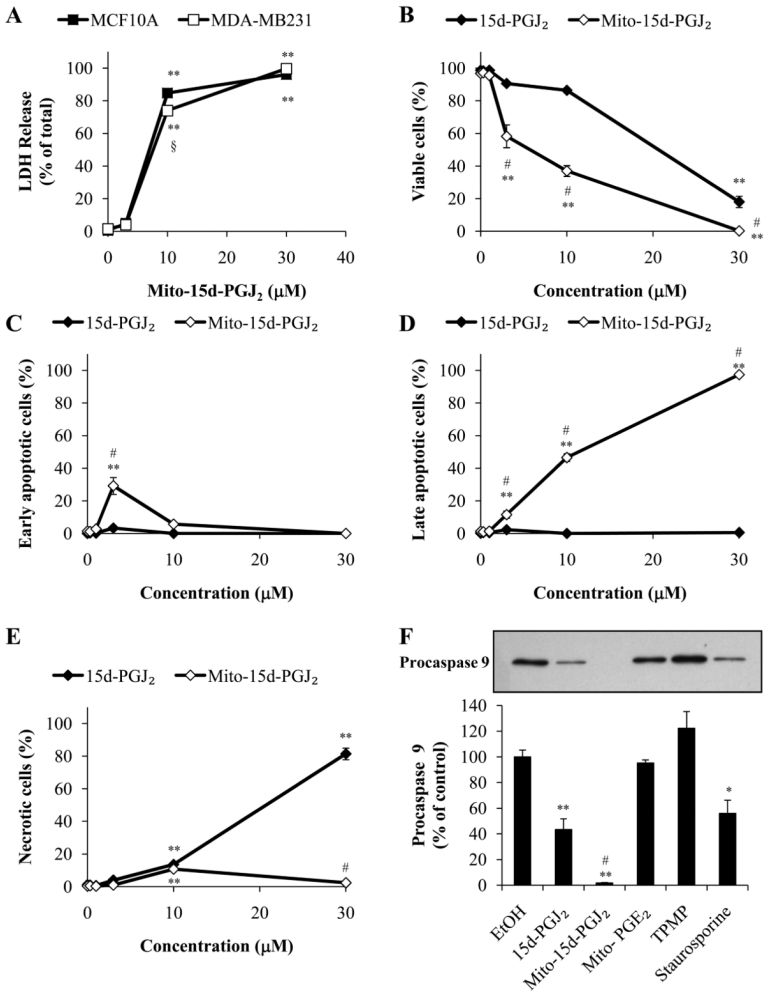

Figure 2. Effect of 15d-PGJ$_2$ and mitochondrial-targeted compounds on cell viability and the induction of apoptosis

Viability of MCF10A and MDA-MB231 cells exposed to increasing concentrations (3–30 μM) of mito-15d-PGJ$_2$ for 16 h was determined by LDH release (**A**). Apoptosis and necrosis after exposure to 15d-PGJ$_2$ or mito-15d-PGJ$_2$ (0.3–30 μM, 16 h) were determined by flow cytometry using PI and Annexin V staining. The percentage of cells which are viable (PI negative and Annexin V negative, **B**), early apoptotic (PI negative and Annexin V positive, **C**), late apoptotic (PI positive and Annexin V positive, **D**), and necrotic (PI positive and Annexin V negative, E) is shown. Caspase 9 activation in MDA-MB231 cells treated with 10 μM 15d-PGJ$_2$, mito-15d-PGJ$_2$, mito-PGE$_2$, or TPMP was assessed using Western blot analysis of Procaspase 9 and quantified (**F**). 1 μM Staurosporine was used as a positive control. Equivalent amounts of protein were loaded for each sample and equal protein loading was confirmed after transfer to nitrocellulose membranes using Ponceau S staining. A representative Western blot is shown. Results represent means ± s.e.m., n = 3. * $p < 0.05$ compared to ethanol (EtOH) vehicle control. ** $p < 0.01$ compared to EtOH vehicle control. # $p < 0.05$ compared to 15d-PGJ$_2$.

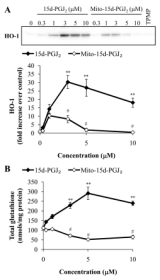

Figure 3. Differential induction of HO-1 and GSH by 15d-PGJ$_2$ and mito-15d-PGJ$_2$

MDA-MB231 cells were treated with increasing concentrations (0.3–10 μM) of 15d-PGJ$_2$ and mito-15d-PGJ$_2$. Cells were treated for 4 h then HO-1 protein levels were determined using Western blot analysis and quantified (**A**). Equivalent amounts of protein were loaded for each sample and equal protein loading was confirmed after transfer to nitrocellulose membranes using Ponceau S staining. A representative Western blot is shown. Cells were treated for 4 h then compound containing media was removed and 0.5% FBS RPMI 1640 was added for an additional 16 h. Cell lysates were then analyzed for total GSH content and values were normalized to protein (**B**). Results represent means ± s.e.m., n = 3. ** $p < 0.01$ compared to ethanol (EtOH) vehicle control. # $p < 0.05$ compared to 15d-PGJ$_2$.

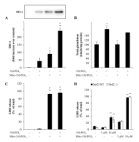

Figure 4. Nrf2-dependence of the regulation of antioxidant expression and cell death

MDA-MB231 cells were pretreated with 1 μM mito-15d-PGJ_2 for 4 h then 1 μM 15d-PGJ_2 was added for an additional 4 h. HO-1 protein levels were determined using Western blot analysis and quantified (**A**). Equivalent amounts of protein were loaded for each sample and equal protein loading was confirmed after transfer to nitrocellulose membranes using Ponceau S staining. A representative Western blot is shown. Cells were treated as described above then compound containing media was removed and 0.5% FBS RPMI 1640 was added for an additional 16 h. Cell lysates were then analyzed for total GSH content and values were normalized to protein (**B**). Viability of MDA-MB231 cells co-incubated with 10 μM mito-15d-PGJ_2 and 3 μM 15d-PGJ_2 for 16 h was determined by LDH release (**C**). Nrf2 wild-type and null murine embryonic fibroblast were treated with 15d-PGJ_2, mito-15d-PGJ_2, or mito-PGE_2 (3 and 10 μM) for 16 h then LDH release was measured (**D**). Results represent means ± s.e.m., n = 3–6. * $p < 0.05$ compared to EtOH vehicle control. ** $p < 0.01$ compared to ethanol (EtOH) vehicle control. # $p < 0.05$ compared to 15d-PGJ_2.

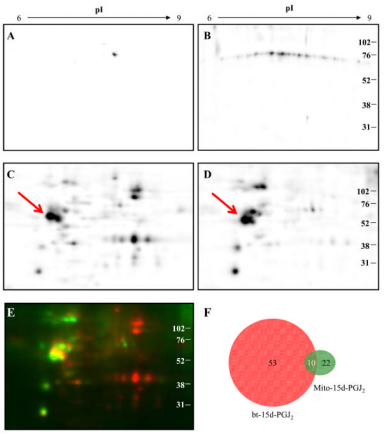

Figure 5. Visualization of bt-15d-PGJ$_2$ and mito-15d-PGJ$_2$ modified proteins by 2D- IEF-SDS-PAGE

Cell lysates from MDA-MB231 cells were separated by 2D-IEF. Ethanol vehicle control (1 h) treated cell lysates were probed using Streptavidin-HRP (**A**) and TPP+ antibody with HRP-conjugated secondary antibody (**B**) to determine background reactivity. Cells were treated (10 μM, 1 h) with bt-15d-PGJ$_2$ (**C**) or mito-15d-PGJ$_2$ (**D**) and protein adducts were detected using Streptavidin-HRP and TPP+ antibody respectively. A merged image of bt-15d-PGJ$_2$ (red) and mito-15d-PGJ$_2$ (green) adduct blots is shown (**E**). Analysis of spot quantity was determined and common and unique spots from bt-15d-PGJ$_2$ and mito-15d-PGJ$_2$ membranes are shown schematically (**F**).

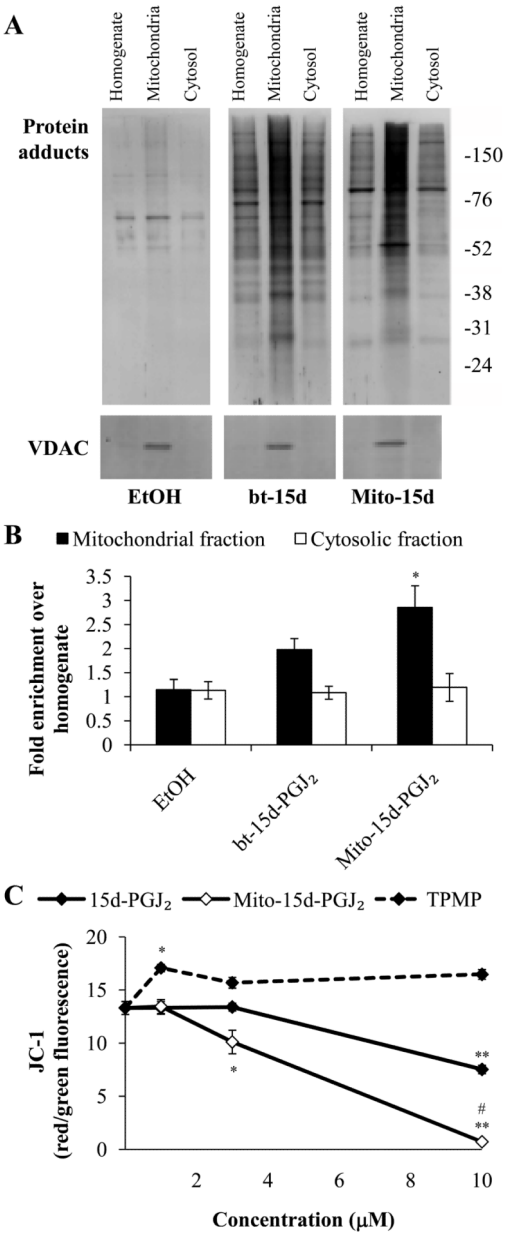

Figure 6. Localization of 15d-PGJ$_2$ and mito-15d-PGJ$_2$ to the mitochondrion and effects on mitochondrial membrane potential (Δ ψ)

MDA-MB231 cells were treated with 10 μM bt-15d-PGJ$_2$ (bt-15d) or mito-15d-PGJ$_2$ (Mito-15d) for 1 h then mitochondrial and cytosolic fractions were prepared and resolved using 10% SDS-PAGE. Adduct formation was detected using an anti-TPP antibody (for mito-15d-PGJ$_2$) or streptavidin-HRP (for bt-15d-PGJ$_2$). ECL+ coupled to horseradish peroxidase was used to detect chemifluorescence protein adducts (**A**). VDAC protein levels were also determined using Western blot analysis to confirm mitochondrial preparation purity. Protein adducts were quantified and expressed as a percent of homogenate (**B**). MDA-MB231 cells were exposed to increasing concentrations (1–10 μM) of 15d-PGJ$_2$, mito-15d-PGJ$_2$, or TPMP for 4 h then Δ ψ was assessed using JC-1 (**C**). Data are represented as the ratio of red/green fluorescence. Results represent means ± s.e.m., n = 3–6.

* $p < 0.05$ compared to ethanol (EtOH) vehicle control. ** $p < 0.01$ compared to EtOH vehicle control. # $p < 0.05$ compared to 15d-PGJ_2.

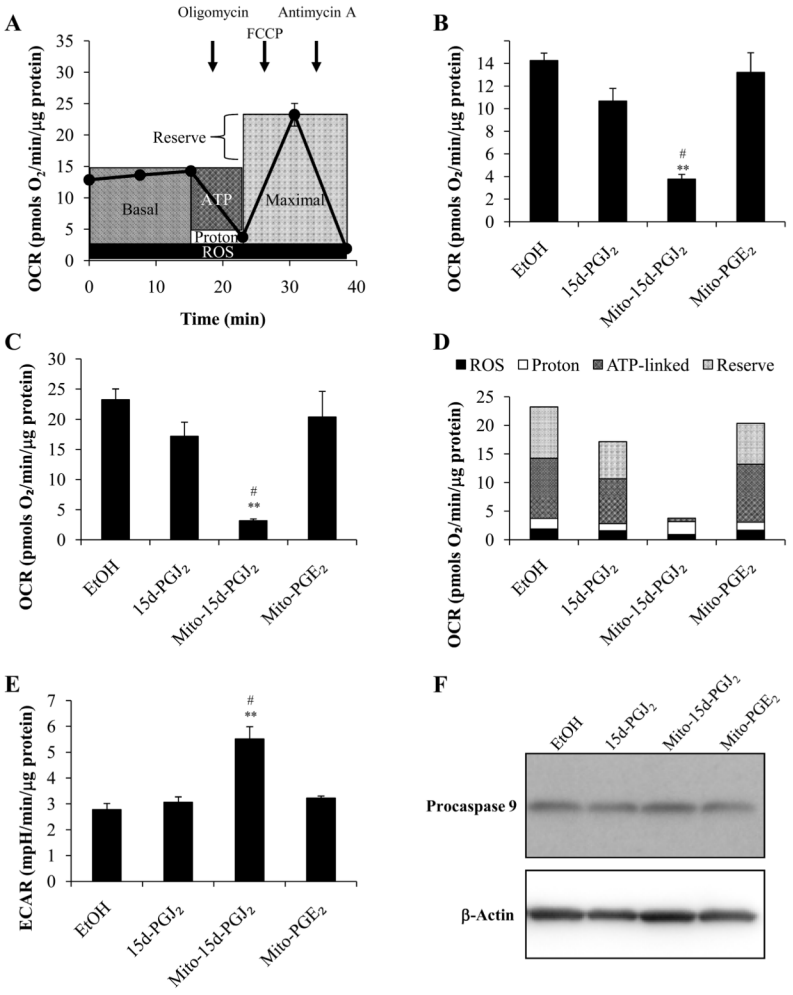

Figure 7. Effect of 15d-PGJ$_2$, mito-15d-PGJ$_2$, and mito-PGE$_2$ on basal and maximal respiration capacity

MDA-MB231 cells were treated for 30 min with of 15d-PGJ$_2$, mito-15d-PGJ$_2$, or mito-PGE$_2$ (10 μM) in specialized 24-well Seahorse Biosciences V7 microplates then bioenergetic function was assessed using the Seahorse XF24 Analyzer. A schematic diagram demonstrating the use of specific inhibitors to determine the sites of cellular oxygen consumption is shown (**A**). Basal oxygen consumption rates (**B**) and maximal oxygen consumption rates (**C**) are shown. The proportion of maximal respiration utilized for ATP-linked respiration (ATP), proton leak (Proton), and ROS formation (ROS), and the reserve respiratory capacity (Reserve) was calculated after measurement of oxygen consumption rates using the Seahorse XF24 Analyzer after sequential injections of oligomycin (0.3 μg/mL), FCCP (1 μM), and antimycin A (10μM) from MDA-MB231 cells treated as previously described (**D**). Basal extracellular acidification rates were measured concomitantly (**E**). Seahorse XF24 Analyzer protocol included 2 min mixing, 2 min waiting, and 3 min measurement times for each measurement. Caspase 9 activation was assessed in samples harvested from a parallel plate treated as previously described using Western blot analysis of Procaspase 9 (**F**). A representative Western blot is shown. Results represent means ± s.e.m., n = 5. ** $p < 0.01$ compared to ethanol (EtOH) vehicle control. # $p < 0.05$ compared to 15d-PGJ$_2$.